

Optimization of Lathe Cutting Parameters Using Taguchi Method and Grey Relational Analysis

Bo-Lin Jian,¹ Cheng-Chi Wang,² Her-Terng Yau,¹
Li-Wei Wu,¹ and An-Hong Tian^{3*}

¹Department of Electrical Engineering, National Chin-Yi University of Technology,
Taichung 41170, Taiwan

²Graduate Institute of Precision Manufacturing, National Chin-Yi University of Technology,
Taichung 41170, Taiwan

³College of Information Engineering, Qijing Normal University, Qijing 655011, China

(Received February 8, 2019; accepted December 27, 2019)

Keywords: Taguchi method, lathe, optimization, grey relational analysis

In the current precision industry, the rapid production of high-quality parts in bulk quantities has led to high competitiveness. In this study, the Taguchi method and grey relational analysis (GRA) approach were used in a practical investigation of precision lathe processing. The purpose was to find optimal parameters for single-target and multitarget cutting. The production of targets of the highest quality was the research focus, with the aim of strengthening the links between this study and the application to the processing industry. Precision, surface roughness, and material removal rate were selected as targets for improvement. The parameters commonly used for lathe processing were set as control factors, and cutting depth, spindle speed, feed rate, and material elongation were set as experimental factors. The results showed that in the cutting of materials, cutting precision was mainly affected by the depth of cut and spindle speed, surface roughness by spindle speed, and the material removal rate by the cutting depth. In a comparison of the quality loss for the same materials using previous parameters, the cutting precision has about 64 to 99% optimization, the surface roughness has 69 to 96% optimization, and the material removal rate has more than 90% optimization. GRA was also employed to analyze the sequences of parameters from the Taguchi experiments to obtain the target relationships and to find the various combinations of factors for improvement.

1. Introduction

The machine tool industry occupies an indispensable position in the development of a country. The precision of processing is continuously increasing in the pursuit of rapid mass production and the quality of products. These aspects of production have become very important and many studies have been conducted to search for ways in which the efficiency and quality of production can be improved. Controllable conditions that have an effect on the quality of the machine turning or milling process include the spindle speed, feed rate, cutting

*Corresponding author: e-mail: tianah@mail.qjnu.edu.cn
<https://doi.org/10.18494/SAM.2020.2674>

fluid, cutting depth, shank angle, and the lathe tools or milling cutters used. Many studies on all these aspects have been conducted,^(1,2) particularly on cutting tool wear.^(3–6) Bharilya *et al.*⁽⁷⁾ used a dynamometer and other devices to investigate the parameters that might reduce cutting force and increase cutting speed. Pislaru *et al.*⁽⁸⁾ used wavelet transformation to identify the resonance frequencies in machine tools and the machine status. Rmili *et al.*⁽⁹⁾ used an acceleration gauge to obtain wear vibration characteristics. This was done to determine whether average power signal processing analysis can be used to develop an automatic detection system for the analysis of tool wear. Cuka and Kim⁽¹⁰⁾ used a dynamometer (a microphone and an accelerometer) to collect signals during cutting and fuzzy clustering to analyze the cutting tool status. To establish the values of parameters in the above research, the costs of data collection and sensors were high, and the material cost of many repeated experiments was also a considerable burden.

The Taguchi method was used in this study to determine the required number of machine experiments and to collect data that can be used for effective analysis. The desired quality characteristics and the experimental factors that may affect quality were selected as reference standards. The standards for a specific item were set using the best combinations that could be found. Pang *et al.*⁽¹¹⁾ used the Taguchi method to optimize processing parameters for specific materials. Das *et al.*⁽¹²⁾ used the grey fuzzy algorithm and Taguchi method to find the best parameters for cutting Al-4.5%Cu-TiC metal composite material on milling machines. Das *et al.*⁽¹³⁾ used fuzzy theory coupled with the Taguchi method to optimize material parameters. Gupta *et al.*⁽¹⁴⁾ also used the Taguchi and fuzzy methods to study parameter optimization using AISI P-20 steel. Asiltürk *et al.*⁽¹⁵⁾ used the Taguchi quality method and response surface methodology (RSM) to conduct research on surface roughness using the medical material Co28Cr6Mo. Li *et al.*⁽¹⁶⁾ also used parameter correlation, RSM, and multiobjective swarm optimization (MOPSO) in the Taguchi method to assist in a search for optimal production efficiency. Ajith Arul Daniel *et al.*⁽¹⁷⁾ used an artificial neural network (ANN) to carry out prediction and parameter optimization research on Taguchi quality and grey relational analysis (GRA) to examine milling machine performance. Thankachan *et al.*⁽¹⁸⁾ used the Taguchi method, GRA, and an ANN to predict and optimize the surface roughness of products made of aluminum alloys and the material removal rate. Tamiloli *et al.*⁽¹⁹⁾ performed GRA using Taguchi factorial experiments and developed an adaptive neuro-fuzzy inference system (ANFIS) model to optimize parameter selection. This showed that GRA can use the signal-to-noise ratio (S/N) obtained from Taguchi experiments for relational analysis. The primary use of the Taguchi method is to reduce the number of experiments, and grey relations produce good results for the analysis of data from short sequences.

However, all these previous studies involved the use of a single material or tool to find the best parameters. Here, we look at the optimization parameters for different materials by examining different common materials processed by the same machine. Workpiece precision, which was not previously a research priority, was a goal in this study and workpiece surface roughness and material removal rate (MRR) were focused on. Ceramic tools, now commonly used in industry, were used in turning experiments with various metals.

2. Methods

To implement the optimized parameters in lathe processing, the Taguchi method and GRA theory were both used, and the experimental flow is shown in Fig. 1.

To explain the framework of the experimental process in detail, experiment-related devices are introduced in Sect. 2.1, and the Taguchi theory and GRA are introduced in Sect. 2.2.

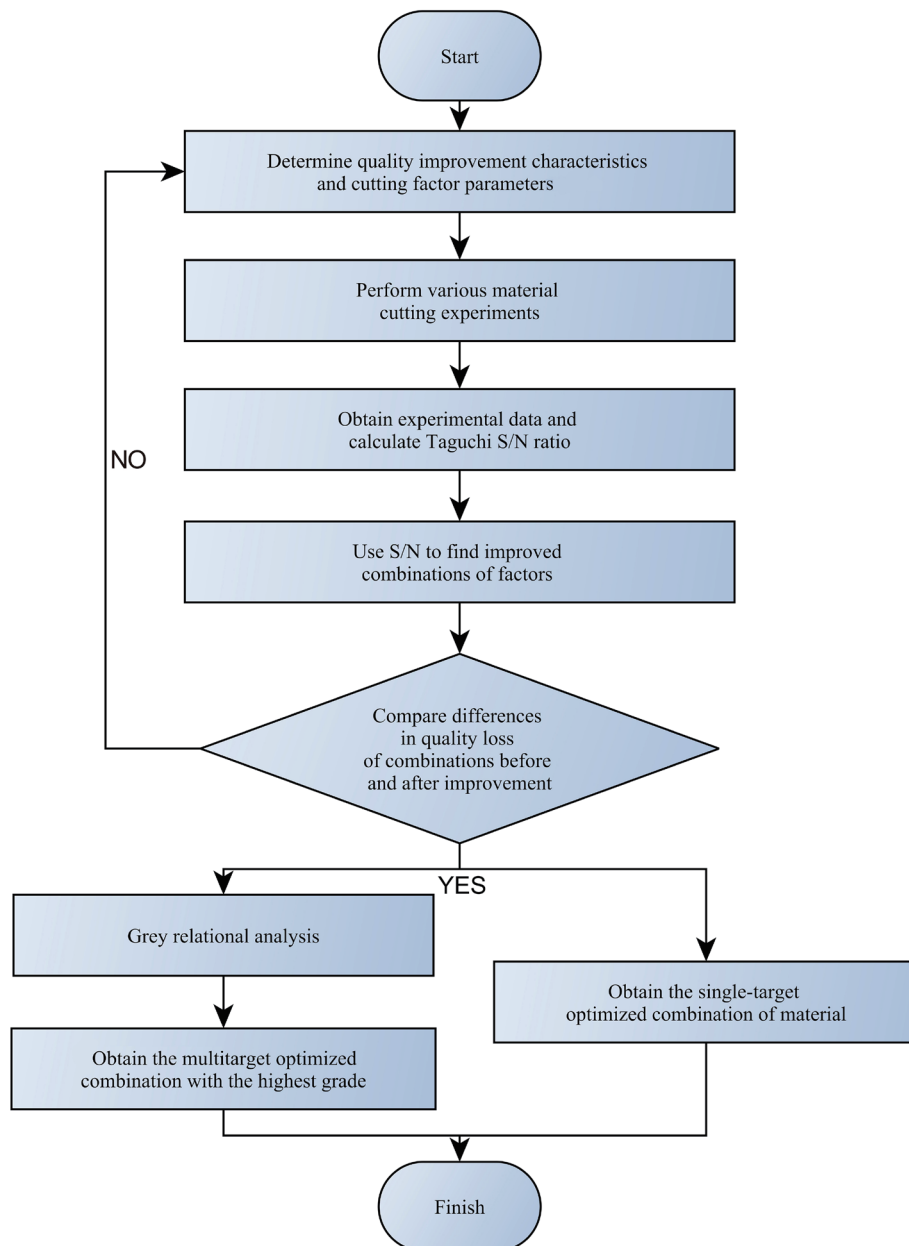


Fig. 1. (Color online) Flowchart of the experiment.

2.1 Specifications of experimental equipment

The machine used was a Mike Machine spherical digital computer numerical control (CNC) (Model MC4200BL), as shown in Fig. 2. The machine had a POSA TAC-10-CY spindle and a SYNTEC 21-TA controller.

The cutting tools used in this study were ceramic and the materials used in the experiments were S45C medium-carbon, S20C low-carbon, SCM415 chromium alloy, 304 stainless, and SCM440 nickel steels, all commonly used in industry. See Table 1 for detailed specifications.

CHAIN ETQNL-2020K16 cutting tools were used. To measure the surface roughness of workpieces, a Mitutoyo SJ-210 surface roughness meter was used. A Carl Zeiss Contura was also used for roughness measurements.

2.2 Taguchi theory and GRA

To reduce the number of experiments needed to find optimal parameters and to make it easy for machine operators to rapidly select them, the Taguchi method⁽²⁰⁾ is used. Genichi Taguchi, in his original work, combined money and loss expressed by quality, not only taking cost into account, but also including consumer and social aspects to arrive at a “loss function”. In



Fig. 2. (Color online) Spherical digital CNC.

Table 1
Workpiece composition in percentages.

Material	Component				
	Medium-carbon steel	Low-carbon steel	Chromium alloy steel	Stainless steel	Nickel steel
C	0.460	0.160	0.13	0.059	0.38
P	0.013	0.015	0.03	0.032	0.03
Mn	0.790	0.410	0.60	1.82	0.60
S	0.007	0.007	0.03	0.0283	0.03
Si	0.220	0.220	0.15	0.46	0.15
Ni	0.020	0.010	0.25	0.54	0.25
Cr	0.140	0.020	0.90	8.10	0.90
Cu	0.010	Tr	—	18.69	0.30
Mo	—	—	0.15	0.12	0.15

product manufacture, the target value is contained in the objective. The purpose of quality is to achieve the target value, and to do this, product variation has to be reduced. Furthermore, to achieve a stable product quality, it is necessary to find the design value parameters. To change these parameters, one must start with the controllable factors involved in production and adjust them without incurring large costs. In the Taguchi method, an orthogonal array is used to rank parameter factor levels. Then, by the standard integration of the factors, the S/N ratios of the combinations can be computed.

The loss function of Taguchi quality is a function of both quality and money. The loss function is expressed by a Tate series.^(20,21)

$$L(y) = K \times (y - m)^2, \quad (1)$$

where m is the target value, y is the characteristic value, and K is the quality loss coefficient (the constant used in measurements).

The improvement targets have expected trends. The status of Taguchi quality can be the larger the better (LTB), the smaller the better (STB), or nominal the best (NTB). LTB is characterized by the largest actual expected value, STB is characterized by the smallest actual expected value, while NTB is between them and is characterized by “expecting the actual value to be close to the target value”. In this study, LTB and STB were the experimental targets. As far as cutting error and surface roughness were concerned, the smaller the error and Ra value, the better the processed workpiece. For the material removal rate, the larger the value, the higher the cutting efficiency.

Owing to prior knowledge of the correlation between the processing control factors and goal achievement, GRA was employed to accomplish the relational analysis of the factors and goals. GRA⁽²²⁾ is an important part of grey theory and is a measurement method for analyzing discrete sequences. Compared with traditional statistical regression, GRA uses a small amount of data and multifactor data to analyze sequence relationships. GRA involves sequence data normalization and can speed up analysis and enhance accuracy. In this study, surface roughness and precision are STB and surface removal rates are LTB. Normalized actions are expressed as follows:

STB:

$$x_i^*(k) = \frac{\max x_i(k) - x_i(k)}{\max x_i(k) - \min x_i(k)}, \quad (2)$$

LTB:

$$x_i^*(k) = \frac{x_i(k) - \min x_i(k)}{\max x_i(k) - \min x_i(k)}. \quad (3)$$

$x_i(k)$ is the largest or smallest in the same quality sequence and current data calculation results. After normalization, the data undergoes sequential grey relational coefficient (GRC) computation.⁽¹⁹⁾ The GRC equation is

$$\xi_i(k) = \frac{\Delta_{min} + \zeta\Delta_{max}}{\Delta_i + \zeta\Delta_{max}}. \quad (4)$$

Here, Δ_i is the difference between the absolute values of the standard sequence and the compared sequence in the same row Δ_{min} , and Δ_{max} is the difference between the maximum and minimum values of the two standards and compared sequences. ζ is the distinguishing coefficient, the function of which is to compare the background object with the object to be tested. Adjusting ζ will only affect the numerical value, not the sequence. Generally, ζ is adjusted to 0.5, but this can be changed to suit actual needs.

Finally, the GRCs are sorted to find the grey relational grade (GRG). The GRG is calculated using the mean of the GRCs, as follows:

$$Y_i = \frac{1}{n} \sum_{k=1}^n \xi_i(k), \quad (5)$$

where n is the output volume in the same row. The computed GRG value was used to rate the sizes of the grades and find the corresponding combination of factor parameters.

The S/N obtained through the Taguchi quality method was computed to obtain the optimal parameters of single targets. The sequence analysis in GRA was then used to analyze Taguchi S/N data and perform relational analysis to obtain multiple targets while improving the parameters.

3. Experimental Results and Discussion

The cutting precision, surface roughness, and MRRS were the quality characteristics in these experiments. Precision is a very important indicator of quality and CNC processing is a large, well-established industrial process. The error reduction leads to a great improvement in product yield rate and reduced costs and is the main reason for this in-depth study of lathe precision. Surface roughness is also a major product indicator and uneven surfaces will affect appearance as well as cause problems between moving contact surfaces. A rough surface will also increase wear, also an integral factor examined in this study. The MRR was calculated using the mass of the workpiece obtained before processing, as described by Shrivastava and Singh.⁽²³⁾

To explain the experimental process framework in detail, the Taguchi experimental process is introduced in Sect. 3.1. Section 3.2 covers the GRA.

3.1 Experimentation using the Taguchi method

With reference to the literature,^(1,8) we varied the cutting depth, spindle speed, feed rate, and material elongation to establish the orthogonal array experimentally. Refer to Table 2 for a comparison of the control factor standards.

Table 2
Control factor standards.

Factor	Standard		
	1	2	3
Cutting depth (mm)	0.1	0.6	1.1
Spindle speed (rpm)	2101	2334	2567
Feed rate (rev)	0.15	0.2	0.25
Elongation (mm)	40	60	80

Table 3
Experimental data—medium-carbon and low-carbon steel quality characteristics.

	Medium-carbon steel			Low-carbon steel		
	Precision error	Surface roughness	MRR	Precision error	Surface roughness	MRR
1	0.013617	1.8886667	0.090909091	0.0085172	1.9026667	0.136363636
2	0.0308	3.251667	0.125	0.00513	3.464	0.222222222
3	0.02955	4.947	0.071428571	0.00493	5.045333	0.214285714
4	0.03207	3.338	0.666666667	0.01036	3.568	0.777777778
5	0.0419	4.979333	0.8125	0.01834	5.105667	0.8125
6	0.01425	1.908	0.65	0.006532	1.915	0.7
7	0.00961	1.698333	1.375	0.00524	5.085333	1.5625
8	0.0053	1.951667	1.15	0.02352	2.031333	1.25
9	0.01391	3.409	1.277777778	0.005562	3.649667	1.333333333

Table 4
Experimental data—chromium alloy, stainless, and nickel steel quality characteristics.

	Chromium alloy steel			Stainless steel			Nickel steel		
	Precision error	Surface roughness	MRR	Precision error	Surface roughness	MRR	Precision error	Surface roughness	MRR
1	0.0148022	1.9753333	0.090909091	0.012118	1.9286667	0.045454545	0.012118	1.9286667	0.045454545
2	0.003659	3.424333	0.166666667	0.0213	3.415333	0.055555556	0.0213	3.415333	0.055555556
3	0.012	4.978667	0.214285714	0.02271	4.875333	0.142857143	0.02271	4.875333	0.142857143
4	0.00375	3.499	0.777777778	0.02483	3.444667	0.722222222	0.02483	3.444667	0.722222222
5	0.01546	4.977	0.875	0.03494	4.936333	0.75	0.03494	4.936333	0.75
6	0.013611	1.912667	0.7	0.01187	1.925	0.65	0.01187	1.925	0.65
7	0.00567	5.099333	1.5625	0.03317	1.910333	1.4375	0.03317	1.910333	1.4375
8	0.032243	1.899	1.3	0.00238	4.910333	1.2	0.00238	4.910333	1.2
9	0.017998	3.347333	1.388888889	0.01503	3.308	1.277777778	0.01503	3.308	1.277777778

The orthogonal array selected in this study was $L_9(3^4)$. Nine experiments in total were performed and cutting was carried out in straight lines. The total cutting depth for each experiment was 30 mm.

Table 3 shows the Taguchi orthogonal experimental data for medium-carbon and low-carbon steels. Table 4 shows the Taguchi orthogonal experimental data for chromium alloy, stainless, and nickel steels. The units of precision error, surface roughness, and MRR are mm, μm , and g/s, respectively.

According to the data measured from the respective targets, LTB and STB S/N ratios are substituted. The data of the materials obtained after computation are shown in Tables 5 and 6.

On the basis of the computed data above, the tables of the target factors of the materials were established. Refer to Tables 7 and 8 for the cutting precision.

Table 5
S/N ratio–medium-carbon and low-carbon steel quality characteristics.

	Medium-carbon steel			Low-carbon steel		
	Precision error	Surface roughness	MRR	Precision error	Surface roughness	MRR
	S/N ratio	S/N ratio	S/N ratio	S/N ratio	S/N ratio	S/N ratio
1	37.318478	-5.523106	-20.8278537	41.394063	-5.587254	-17.3060285
2	30.22868	-10.2421	-18.0617997	45.80166	-10.7916	-13.0642502
3	30.59003	-13.8868	-22.9225607	46.14394	-14.0578	-13.3801356
4	29.8778	-10.4697	-3.52182518	39.6894	-11.0485	-2.18288938
5	27.55548	-13.9434	-1.80353260	34.73072	-14.161	-1.80353260
6	36.92665	-5.61157	-3.74173286	43.69956	-5.64338	-3.0980392
7	40.34466	-4.60046	2.766053963	45.62001	-14.1264	3.87640052
8	45.5153	-5.80811	1.213956807	32.57124	-6.15562	1.93820026
9	37.13383	-10.6525	2.129106618	45.09538	-11.2451	2.498774732

Table 6
S/N ratio–chromium alloy, stainless, and nickel steel quality characteristics.

	Chromium alloy steel			Stainless steel			Nickel steel		
	Precision error	Surface roughness	MRR	Precision error	Surface roughness	MRR	Precision error	Surface roughness	MRR
	S/N ratio	S/N ratio	S/N ratio	S/N ratio	S/N ratio	S/N ratio	S/N ratio	S/N ratio	S/N ratio
1	36.593484	-5.912808	-20.8278537	38.331118	-5.705143	-26.8484536	26.88675818	-6.16132330	-14.8072537
2	48.73319	-10.6915	-15.5630250	33.43109	-10.6687	-25.1054501	29.57641861	-11.5918615	-15.5630250
3	38.41598	-13.9423	-13.3801356	32.87418	-13.7601	-16.9019608	31.57267149	-14.2153184	-10.8813608
4	48.53031	-10.8789	-2.18288938	32.10034	-10.7429	-2.82658305	30.1645791	-11.2791093	-1.02305044
5	36.2156	-13.9394	-1.15983894	29.13375	-13.8681	-2.49877473	34.5503575	-14.3534100	-0.56057447
6	37.32252	-5.63279	-3.0980392	38.51394	-5.68861	-3.74173286	26.40484233	-6.13278882	-1.93820026
7	44.92834	-14.1503	3.87640052	29.58562	-5.62218	3.152157067	27.57732637	-14.3976694	4.54487563
8	29.8312	-5.5705	2.278867046	52.48051	-13.8222	1.583624921	23.1290701	-6.64472831	2.60667537
9	34.89566	-10.494	2.853350071	36.46074	-10.3913	2.129106618	26.40941923	-11.5467716	3.521825181

Table 7
Factor results–medium-carbon and low-carbon steel cutting errors.

Standard	Factor							
	Medium-carbon steel				Low-carbon steel			
	A	B	C	D	A	B	C	D
1	32.71239619	35.84698009	39.92014298	34.00259808	44.44655548	42.23448879	39.22162283	40.40672078
2	31.45331268	34.43315718	32.41344036	35.83333092	39.37322635	37.70120702	43.52881237	45.04041069
3	40.99793091	34.8835025	32.83005644	35.32771078	41.09554296	44.97962899	42.16488959	39.46819332
Difference	9.544618227	1.413822912	7.506702624	1.830732838	5.073329123	7.278421967	4.307189537	5.572217367

Table 8
Factor results–chromium alloy, stainless, and nickel steel cutting errors.

Standard	Factor							
	Chromium alloy steel				Stainless steel			
	A	B	C	D	A	B	C	D
1	41.24754948	43.3507099	34.58240139	35.90158282	34.87879543	33.3390262	43.10852281	34.64187024
2	40.68947635	38.25999752	44.0530511	43.66134808	33.24934134	38.34845045	33.99739007	33.84355002
3	36.55173333	36.87805174	39.85330667	38.92582825	39.50895968	35.9496198	30.53118358	39.15167619
Difference	4.695816146	6.472658155	9.470649712	7.759765263	6.259618343	5.009424247	12.57733923	5.30812617

Standard	Factor			
	Nickel steel			
	A	B	C	D
1	29.34528276	28.20955455	25.47355687	29.28217831
2	30.37325964	29.08528207	28.71680565	27.85286244
3	25.7052719	28.12897768	31.23345179	28.28877356
Difference	4.667987743	0.95630439	5.759894916	1.429315868

The obtained factor values were imported into software and presented in resonance diagrams to identify the difference in S/N ratio between various factor standards. Figure 3 shows cutting precision resonance diagrams.

Tables 9 and 10 are the tabulated factor results of surface roughness. Figure 4 shows surface roughness resonance diagrams.

Tables 11 and 12 are the factor results of MRRs. Figure 5 shows MRR resonance diagrams.

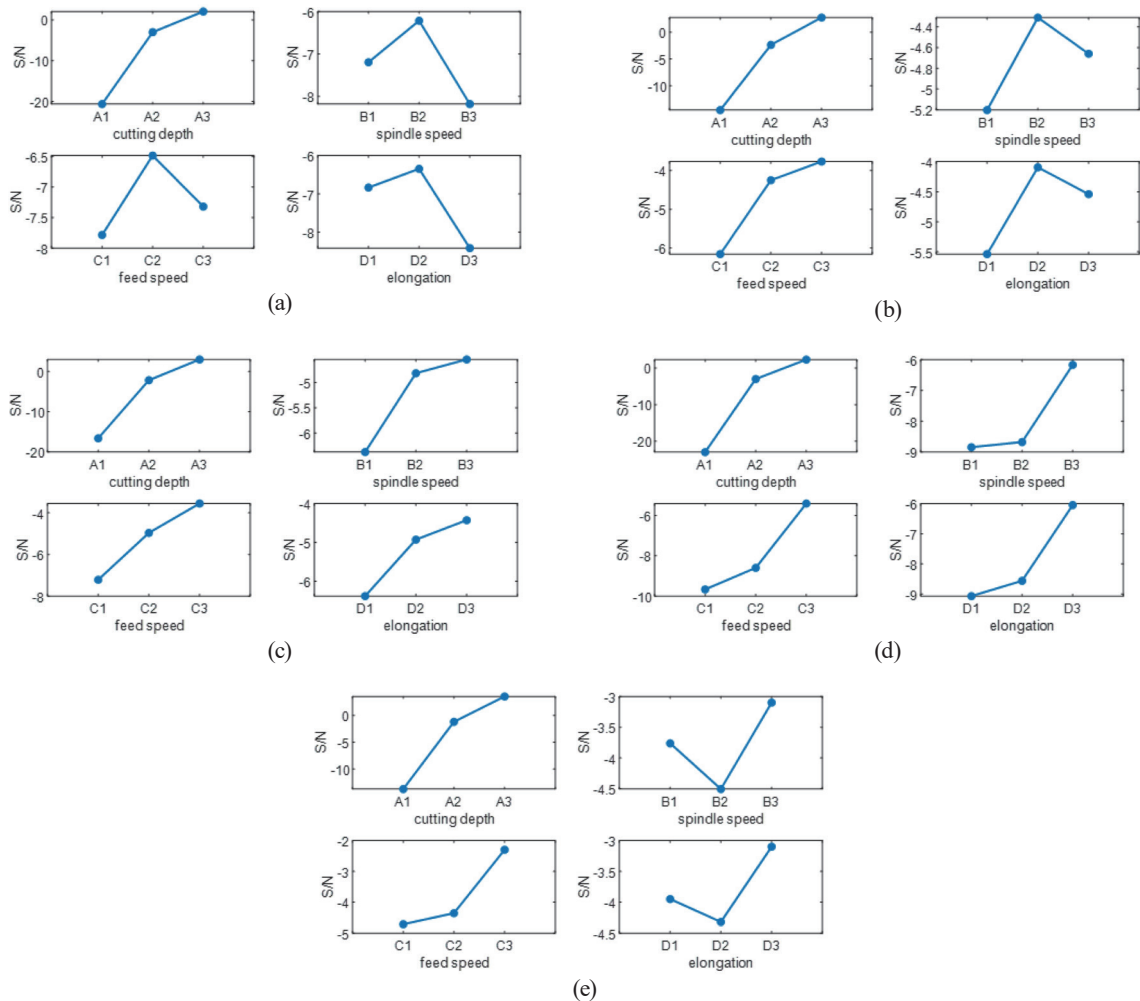


Fig. 3. (Color online) Resonance diagrams of cutting errors: (a) medium-carbon, (b) low-carbon, (c) chromium alloy, (d) stainless, and (e) nickel steels.

Table 9
Factor results—medium-carbon and low-carbon steel surface roughnesses.

Standard	Factor							
	Medium-carbon steel				Low-carbon steel			
	A	B	C	D	A	B	C	D
1	-9.884021632	-6.864430543	-5.647595537	-10.03969011	-10.14553638	-10.25404654	-5.795417888	-10.33112246
2	-10.00823935	-9.997885761	-10.45479568	-6.81804882	-10.28430721	-10.36941024	-11.02837287	-10.18710725
3	-7.02037053	-10.05031521	-10.8102403	-10.05489258	-10.50902548	-10.31541229	-14.11507832	-10.42063937
Difference	2.987868824	3.18588467	5.162644759	3.236843763	0.363489094	0.115363703	8.319660427	0.233532122

Table 10
Factor results—chromium alloy, stainless, and nickel steel surface roughnesses.

Standard	Factor							
	Chromium alloy steel				Stainless steel			
	A	B	C	D	A	B	C	D
1	-10.18219651	-10.31398491	-5.705364309	-10.11537997	-10.04463057	-7.356756872	-8.405325888	-9.988181026
2	-10.15033915	-10.06712426	-10.68812625	-10.1581915	-10.09988276	-12.78632367	-10.600972	-7.326486563
3	-10.07158219	-10.02300868	-14.01062729	-10.13054638	-9.945237529	-9.946670327	-11.08345298	-12.77508328
Difference	0.110614314	0.290976234	8.305262977	0.042811526	0.154645236	5.429566795	2.678127089	5.448596715

Standard	Factor			
	Nickel steel			
	A	B	C	D
1	-10.65616776	-10.61270069	-6.312946812	-10.68716834
2	-10.58843606	-10.86333329	-11.47258082	-10.70743993
3	-10.86305648	-10.63162631	-14.32213267	-10.71305203
Difference	0.274620415	0.250632598	8.009185854	0.025883689

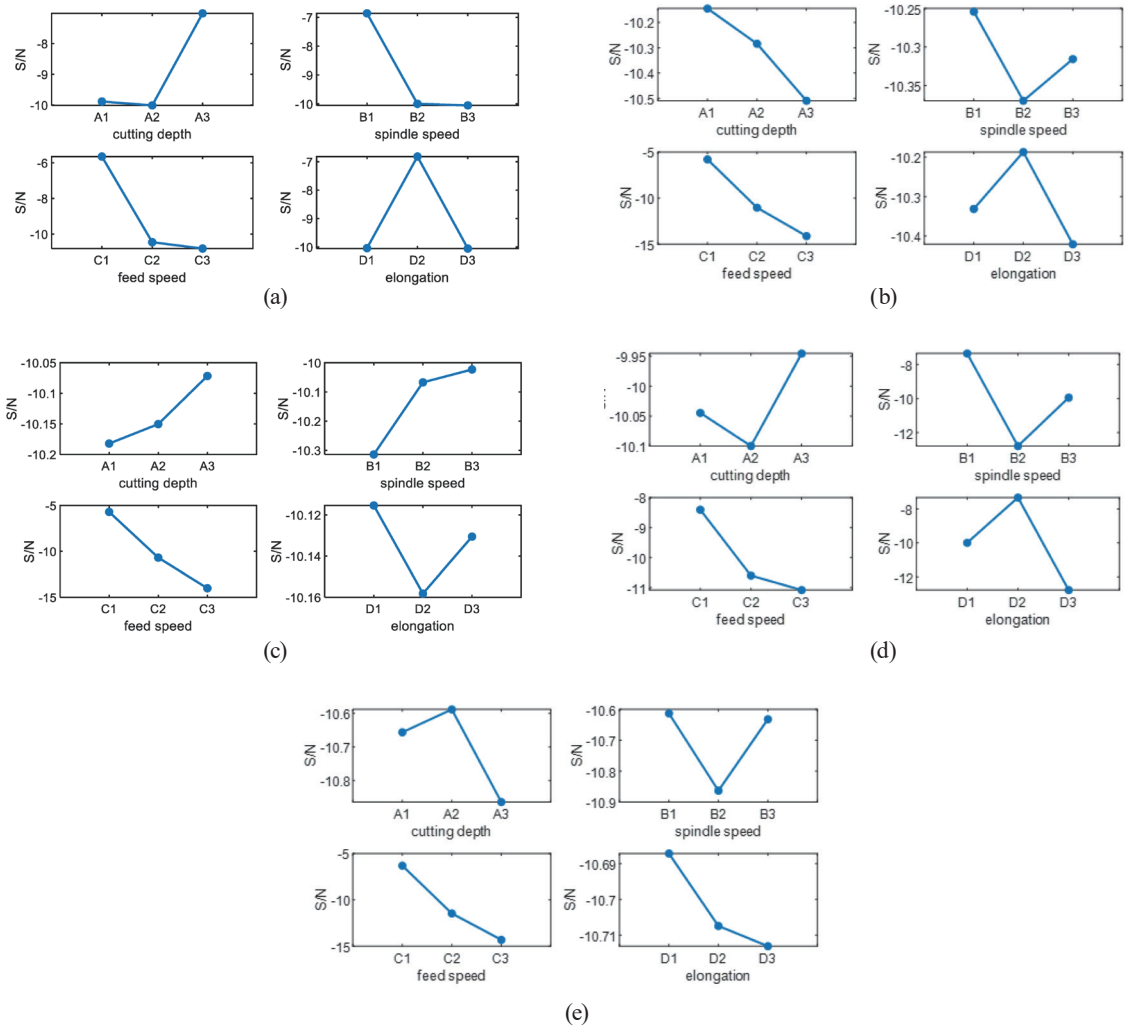


Fig. 4. (Color online) Resonance diagrams of surface roughness: (a) medium-carbon, (b) low-carbon, (c) chromium alloy, (d) stainless, and (e) nickel steels.

Table 11
Factor results–medium–carbon and low–carbon steel MRRs.

Standard	Factor							
	Medium-carbon steel				Low-carbon steel			
	A	B	C	D	A	B	C	D
1	-20.60407139	-7.19454164	-7.785209921	-6.834093231	-14.58347147	-5.204172463	-6.155289154	-5.536928799
2	-3.022363552	-6.21712518	-6.484839434	-6.345826215	-2.361487065	-4.309860874	-4.249454977	-4.095296318
3	2.036372463	-8.178395654	-7.320013119	-8.410143029	2.771125171	-4.659800029	-3.769089235	-4.541608249
Difference	22.64044385	1.961270474	1.300370487	2.064316815	17.35459664	0.894311589	2.386199919	1.441632481

Table 12
Factor results–chromium alloy, stainless, and nickel steel MRRs.

Standard	Factor							
	Chromium alloy steel				Stainless steel			
	A	B	C	D	A	B	C	D
1	-16.59033811	-6.37811419	-7.215675286	-6.37811419	-22.95195484	-8.840959868	-9.668853854	-9.072707243
2	-2.146922509	-4.814665634	-4.964188108	-4.928221229	-3.022363552	-8.673533304	-8.600975513	-8.565008634
3	3.002872546	-4.541608249	-3.554524679	-4.428052654	2.288296202	-6.171529016	-5.416192822	-6.048306312
Difference	19.59321066	1.836505941	3.661150606	1.950061537	25.24025104	2.669430852	4.252661032	3.024400932

Standard	Factor			
	Nickel steel			
	A	B	C	D
1	-13.75054656	-3.761809536	-4.712926227	-3.948667694
2	-1.173941727	-4.50564137	-4.354750092	-4.318783213
3	3.55779206	-3.099245322	-2.29901991	-3.099245322
Difference	17.30833862	1.406396048	2.413906317	1.219537891

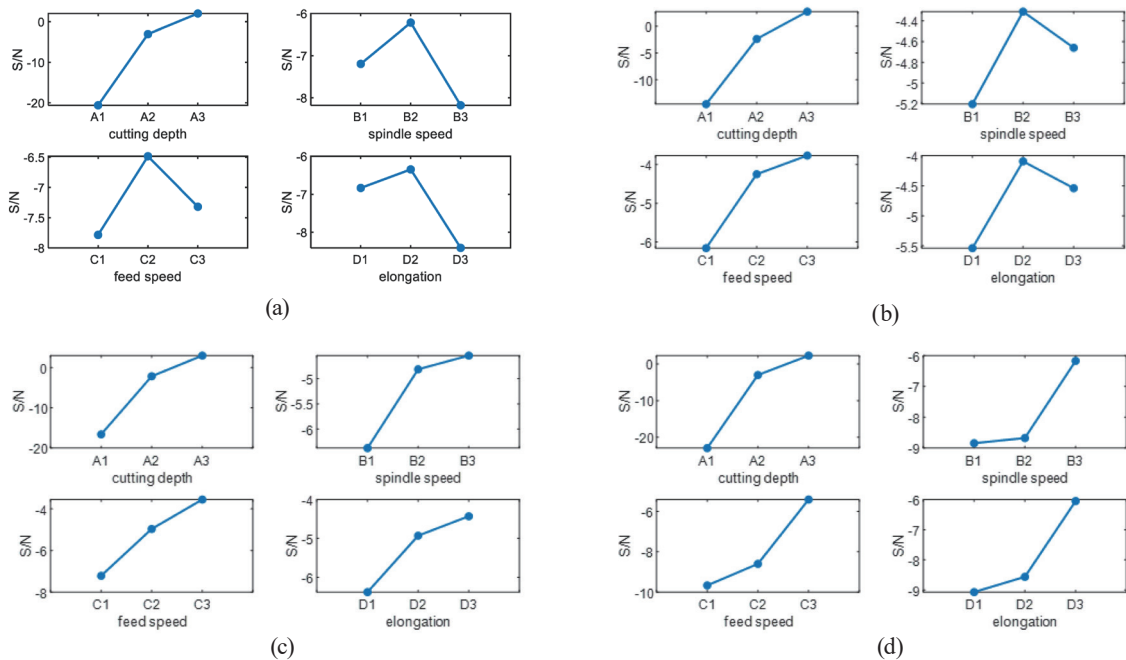


Fig. 5. (Color online) Resonance diagrams of MRRs: (a) medium-carbon, (b) low-carbon, (c) chromium alloy, and (d) stainless steels.

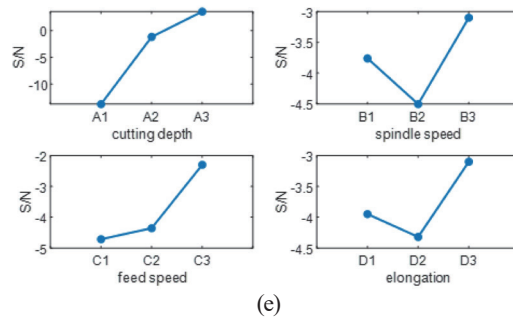


Fig. 5. (Color online) (Continued) Resonance diagrams of MRRs: (e) nickel steel.

Table 13

Best configuration combinations of material factors.

	Medium-carbon steel	Low-carbon steel	Chromium alloy steel	Stainless steel	Nickel steel
Cutting precision	A3B1 C1D2	A1B3 C2D2	A1B1 C2D2	A3B2 C1D3	A2B2 C3D1
Surface roughness	A3B1 C1D2	A1B1 C1D2	A3B3 C1D1	A3B1 C1D2	A2B1 C1D1
Material removal rate	A3B2 C2D2	A3B2 C3D2	A3B3 C3D3	A3B3 C3D3	A3B3 C3D3

Table 14

Reduction percentages of quality loss for different material combinations.

	Medium-carbon steel (%)	Low-carbon steel (%)	Chromium alloy steel (%)	Stainless steel (%)	Nickel steel (%)
Cutting precision	98.61	65.59	96.22	99.13	64.52
Surface roughness	96.10	71.41	69.04	82.40	70.12
Material removal rate	99.69	98.91	99.49	99.92	99.04

The Taguchi quality calculation shows the impact of the factor standards of the materials from which the factor standard combinations most suitable for the targets were selected. We computed the quality loss of the originally set factor combinations and the improved best combinations to determine the amount of loss reduction. The previous experimental parameters and materials were set as A1B3C2D1, and the improved factor configuration is shown in Table 13.

The results of the computed quality loss are shown in Table 14. This table shows that the best combinations can reduce the quality loss of many preset combinations. The best parameters can be obtained to carry out parameter optimization on single targets.

3.2 GRA

Taguchi quality involves the computation of S/N to determine which experimental combination of factors is optimal for single targets. Here, the sequence data under the Taguchi orthogonal experiment was used to perform GRA. The target quality underwent multitarget optimization. Tables 15 and 16 show the normalized S/N ratios and respective target sequences

obtained after GRC and GRG analyses. The material analysis results are shown in Tables 17 and 18.

Observations of the material grade show that a higher GRG produces a higher overall impact. It was found that the eighth combination is the best for medium-carbon steel, the sixth combination is best for low-carbon steel, the eighth combination is best for chromium alloy steel, the seventh combination is best for stainless steel, and the eighth combination is best for nickel steel. Thus, the eighth combination produces beneficial results for the optimization of various materials.

Table 15
Normalized S/N data—medium-carbon and low-carbon steel data.

	Medium-carbon steel			Low-carbon steel		
	Precision error	Surface roughness	MRR	Precision error	Surface roughness	MRR
1	0.543602	0.901247	0.081542	0.650042	1	0
2	0.148843	0.39616	0.189218	0.974782	0.39299	0.20025
3	0.168963	0.006058	0	1	0.012037	0.185337
4	0.129306	0.371799	0.755227	0.524447	0.363027	0.713947
5	0	0	0.822116	0.159105	0	0.731856
6	0.521785	0.891778	0.746666	0.819905	0.993454	0.670744
7	0.7121	1	1	0.961398	0.004036	1
8	1	0.870742	0.93958	0	0.933709	0.9085
9	0.533321	0.352234	0.975205	0.922745	0.340096	0.934964

Table 16
Normalized S/N data—chromium alloy, stainless, and nickel steel data.

	Chromium alloy steel			Stainless steel			Nickel steel		
	Precision error	Surface roughness	MRR	Precision error	Surface roughness	MRR	Precision error	Surface roughness	MRR
1	0.357755	0.960103	0	0.393946	0.989939	0	0.329007	0.996548	0.037586
2	1	0.403133	0.213114	0.184066	0.387998	0.058099	0.564503	0.339486	0
3	0.454173	0.024243	0.301475	0.160212	0.013097	0.331543	0.739286	0.022063	0.232827
4	0.989267	0.381291	0.754727	0.127066	0.379	0.800713	0.616	0.377327	0.723098
5	0.337763	0.024581	0.796139	0	0	0.811639	1	0.005355	0.746097
6	0.396324	0.99274	0.717683	0.401777	0.991944	0.770208	0.286813	1	0.677586
7	0.798706	0	1	0.019355	1	1	0.389471	0	1
8	0	1	0.935334	1	0.005566	0.947717	0	0.938058	0.90361
9	0.267933	0.426152	0.958588	0.313833	0.421639	0.965899	0.287214	0.344941	0.949122

Table 17
GRG—medium-carbon and low-carbon steels.

	Medium-carbon steel					Low-carbon steel				
	GRC				Rank	GRC				Rank
	Cutting precision	Ra	MRR	GRG		Cutting precision	Ra	MRR	GRG	
1	0.522795	0.835068	0.352496	0.57012	5	0.588264	1	0.333333	0.640533	5
2	0.370053	0.452964	0.381452	0.40149	8	0.951985	0.451667	0.384689	0.596114	6
3	0.375647	0.334685	0.333333	0.347888	9	1	0.33603	0.380326	0.572118	7
4	0.364779	0.443184	0.671346	0.493103	6	0.51253	0.439764	0.63609	0.529461	8
5	0.333333	0.333333	0.73759	0.468085	7	0.372885	0.333333	0.65092	0.452379	9
6	0.511135	0.822068	0.663717	0.66564	3	0.735191	0.987077	0.60295	0.775073	1
7	0.634598	1	1	0.878199	2	0.92833	0.334233	1	0.754187	2
8	1	0.794587	0.892189	0.895592	1	0.333333	0.882938	0.845308	0.687193	4
9	0.517235	0.435629	0.952753	0.635206	4	0.866168	0.43107	0.884899	0.727379	3

Table 18
GRG–chromium alloy, stainless, and nickel steels.

	Chromium alloy steel					Stainless steel				
	GRC			GRG	Rank	GRC			GRG	Rank
	Cutting precision	Ra	MRR			Cutting precision	Ra	MRR		
1	0.437735	0.926103	0.333333	0.565723	7	0.452058	0.980275	0.333333	0.588555	5
2	1	0.455844	0.388535	0.614793	5	0.379958	0.449639	0.346764	0.392121	8
3	0.478091	0.338809	0.417179	0.41136	9	0.373193	0.33627	0.427915	0.379126	9
4	0.978985	0.446944	0.670895	0.698941	2	0.364184	0.44603	0.715014	0.508409	6
5	0.430205	0.338887	0.710367	0.493153	8	0.333333	0.333333	0.726364	0.464343	7
6	0.453032	0.985688	0.639127	0.692615	3	0.455281	0.984143	0.685127	0.708184	3
7	0.712968	0.333333	1	0.6821	4	0.337691	1	1	0.77923	1
8	0.333333	1	0.885479	0.739604	1	1	0.334575	0.905332	0.746636	2
9	0.405822	0.465615	0.923511	0.598316	6	0.421526	0.463667	0.936153	0.607115	4

	Nickel steel				
	GRC			GRG	Rank
	Cutting precision	Ra	MRR		
1	0.426988	0.993142	0.3419	0.587344	5
2	0.534475	0.430843	0.333333	0.432884	9
3	0.657278	0.338309	0.394579	0.463389	8
4	0.565611	0.445366	0.643581	0.551519	7
5	1	0.334528	0.663216	0.665914	3
6	0.412138	1	0.607966	0.673368	2
7	0.450236	0.333333	1	0.594523	4
8	0.333333	0.889772	0.838378	0.687161	1
9	0.412274	0.432878	0.907642	0.584265	6

The Taguchi quality experimental method was used to find a single optimization target combination relative to the previous combination. Thus, with the assistance of GRA, the machine users can select a “single target” or search for “optimal parameters for multiple optimizations”.

4. Conclusion

We presented the results of an investigation of optimal parameters for the lathe machining of several different materials using the Taguchi method and GRA. The experimental results show the impacts of the cutting precision targets of various materials, with cutting depth and spindle speed having the greatest impacts. Spindle speed affected surface roughness, and cutting depth affected the material removal rate. These factors can be used by machine operators to adjust and improve target selection. The optimal parameter combinations found in this study reduced quality loss more significantly than previous combinations. This achieved the purpose of the search for optimized parameters. In the future, other directions, such as the analysis of variance (ANOVA) to derive more specific selections and enhance parameter optimization, could be investigated.

Acknowledgments

The authors acknowledge with gratitude a funding grant from the Ministry of Science and Technology for the project “Domestic Lathe Machine Tool Spindle Peripheral Smart Functional Technology Development” (project No. MOST 108-2218-E-167-001). This work was also financially supported by the Teacher Education Research Project of Qujing Normal University under Grant No. 2019JZ001.

References

- 1 K. Venkatesh, M. C. Zhou, and R. J. Caudill: *J. Intell. Manuf.* **8** (1997) 215. <https://doi.org/10.1023/A:1018573224739>
- 2 D. E. Dimla: *Int. J. Mach. Tools Manuf.* **40** (2000) 1073. [https://doi.org/10.1016/s0890-6955\(99\)00122-4](https://doi.org/10.1016/s0890-6955(99)00122-4)
- 3 A. Siddhpura and R. Paurobally: *Int. J. Adv. Manuf. Technol.* **65** (2013) 371. <https://doi.org/10.1007/s00170-012-4177-1>
- 4 D. Choi, W. T. Kwon, and C. N. Chu: *Int. J. Adv. Manuf. Technol.* **15** (1999) 305. <https://doi.org/10.1007/s001700050071>
- 5 D. Yan, T. I. El-Wardany, and M. A. Elbestawi: *Int. J. Mach. Tools Manuf.* **35** (1995) 383. [https://doi.org/10.1016/0890-6955\(94\)e0021-a](https://doi.org/10.1016/0890-6955(94)e0021-a)
- 6 M. Nouri, B. K. Fussell, B. L. Ziniti, and E. Linder: *Int. J. Mach. Tools Manuf.* **89** (2015) 1. <https://doi.org/10.1016/j.ijmachtools.2014.10.011>
- 7 R. K. Bharilya, R. Malgaya, L. Patidar, R. K. Gurjar, and A. K. Jha: *Mater. Today: Proc.* **2** (2015) 2300. <https://doi.org/10.1016/j.matpr.2015.07.268>
- 8 C. Pislaru, J. M. Freeman, and D. G. Ford: *Int. J. Mach. Tools Manuf.* **43** (2003) 987. [https://doi.org/10.1016/S0890-6955\(03\)00104-4](https://doi.org/10.1016/S0890-6955(03)00104-4)
- 9 W. Rmili, A. Ouahabi, R. Serra, and R. Leroy: *Measurement* **77** (2016) 117. <https://doi.org/10.1016/j.measurement.2015.09.010>
- 10 B. Cuka and D. W. Kim: *Rob. Comput. Integr. Manuf.* **47** (2017) 22. <https://doi.org/10.1016/j.rcim.2016.12.009>
- 11 J. S. Pang, M. N. M. Ansari, O. S. Zaroog, M. H. Ali, and S. M. Sapuan: *HBRC J.* **10** (2014) 138. <https://doi.org/10.1016/j.hbrj.2013.09.007>
- 12 B. Das, S. Roy, R. N. Rai, and S. C. Saha: *Eng. Sci. Technol.* **19** (2016) 857. <https://doi.org/10.1016/j.jestch.2015.12.002>
- 13 B. Das, S. Roy, R. N. Rai, and S. C. Saha: *Eng. Sci. Technol.* **19** (2016) 279. <https://doi.org/10.1016/j.jestch.2015.08.002>
- 14 A. Gupta, H. Singh, and A. Aggarwal: *Expert Syst. Appl.* **38** (2011) 6822. <https://doi.org/10.1016/j.eswa.2010.12.057>
- 15 I. Asiltürk, S. Neseli, and M. A. Ince: *Measurement* **78** (2016) 120. <https://doi.org/10.1016/j.measurement.2015.09.052>
- 16 C. B. Li, Q. G. Xiao, Y. Tang, and L. Li: *J. Clean Prod.* **135** (2016) 263. <https://doi.org/10.1016/j.jclepro.2016.06.097>
- 17 S. Ajith Arul Daniel, R. Pugazhenthii, R. Kumar, and S. Vijayananth: *Def. Technol.* **15** (2019) 545. <https://doi.org/10.1016/j.dt.2019.01.001>
- 18 T. Thankachan, K. S. Prakash, R. Malini, S. Ramu, P. Sundararaj, S. Rajandran, D. Rammasamy, and S. Jothi: *Appl. Surf. Sci.* **472** (2019) 22. <https://doi.org/10.1016/j.apsusc.2018.06.117>
- 19 N. Tamiloli, J. Venkatesan, and B. V. Ramnath: *Measurement* **84** (2016) 68. <https://doi.org/10.1016/j.measurement.2016.02.008>
- 20 R. L. Edgeman: *Technometrics* **34** (1992) 230. <https://dx.doi.org/10.1080/00401706.1992.10484920>
- 21 F. C. Wu: *Int. J. Adv. Manuf. Technol.* **20** (2002) 749. <https://doi.org/10.1007/s001700200233>
- 22 J. W. K. Chan and T. K. L. Tong: *Mater. Des.* **28** (2007) 1539. <https://doi.org/10.1016/j.matdes.2006.02.016>
- 23 Y. Shrivastava and B. Singh: *Eur. J. Mech. A Solids* **70** (2018) 238. <https://doi.org/10.1016/j.euromechsol.2018.03.009>

About the Authors



Bo-Lin Jian received his B.S. degree from the Department of Electrical Engineering, National Formosa University in 2009 and his degree M.S. in materials science and engineering from the National Taiwan University of Science and Technology in 2011. His Ph.D. degree was awarded by the Department of Aeronautics and Astronautics, National Cheng Kung University in 2017. He is an assistant professor in the Department of Electrical Engineering, National Chin-Yi University of Technology, Taichung, Taiwan. His current research interests include signal and image processing, machine learning, and control systems. (BoLin@ncut.edu.tw)



Cheng-Chi Wang serves as a distinguished professor and also the dean of the Graduate Institute of Precision Manufacturing in National Chin-Yi University of Technology in Taiwan. His current research involves intelligent machining and manufacturing, nonlinear dynamic analysis, simulation and optimization, air lubrication system and signal processing. (wcc@ncut.edu.tw)



Her-Terng Yau received his B.S. degree from National Chung Hsing University, Taichung, Taiwan, in 1994 and his M.S. and Ph.D. degrees from National Cheng Kung University, Tainan, Taiwan, in 1996 and 2000, respectively, all in mechanical engineering. He is currently a professor in the Department of Electrical Engineering, National Chin-Yi University of Technology, Taichung, Taiwan. His research interests include energy converter control, system control of mechatronics, nonlinear system analysis, and control. He is the author of more than 150 research articles on a wide variety of topics in mechanical and electrical engineering. (htyau@ncut.edu.tw)



Li-Wei Wu received his B.S. and M.S. degrees from the Department of Electrical Engineering, National Chin-Yi University of Technology in 2017 and 2019, respectively. (ff9456gdgs@gmail.com)



An-Hong Tian received her B.S. and M.S. degrees from Chongqing University of Posts and Telecommunications, China, in 2007 and 2010, respectively. From 2011 to 2016, she was a lecturer at Qujing Normal University, China. Since 2017, she has been an associate professor at Qujing Normal University. Her research interests are in remote sensing, wireless navigation, and artificial intelligence. (tianah@mail.qjnu.edu.cn)